Effects of Various Uncertainty Sources on Automatic Generation Control Systems

D. Apostolopoulou, Y. C. Chen, J. Zhang, A. D. Domínguez-García, and P. W. Sauer
Department of Electrical and Computer Engineering
University of Illinois at Urbana-Champaign
Urbana, Illinois 61801
Email: {apostol2, chen267, jzhang67, aledan, psauer}@illinois.edu

Abstract—In power systems, the automatic generation control (AGC) system is responsible for maintaining the nominal system frequency and the scheduled real power interchange between balancing areas. This paper proposes a framework to evaluate the effects of uncertainty arising from renewable-based electricity generation and noise in communication channels on the AGC system performance. To this end, we introduce a unified stochastic differential equation (SDE) model that includes power system dynamics and the AGC system (including the communication network on which its operation relies). We propagate the uncertainty from renewable-based resources and communication channel noise through the SDE model and investigate the resulting effect on AGC system performance. The proposed ideas are illustrated through a 4-bus test system.

Introduction

When operating the electrical grid, an objective is to reliably meet electricity demand through a series of control systems. One such system is the automatic generation control (AGC), which is responsible for maintaining the nominal system frequency and the real power interchange between balancing authority (BA) areas to the scheduled quantities. This task is becoming more challenging due to the radical transformations occurring in the structure and functionality of power systems. These transformations are enabled by the integration of new technologies, such as advanced communication and power electronics devices, and the deep penetration of renewable resources. These new technologies, however, raise new challenges in the reliable operation of power systems [1]. For example, wind generation is not only intermittent and highly variable, it also introduces an additional source of uncertainty to power system operations. As a consequence, independent system operators (ISOs) must schedule adequate electric supply from traditional generators on AGC to manage larger net system load variations caused by increased levels of wind generation.

The AGC system accepts measurements of the real power interchange between BA areas, the area's frequency and the generators' output as inputs from field devices and processes them to obtain the output control signals, i.e., generator control commands. The combination of uncertainty from renewable resources and noise from communication channels, however, may affect AGC system performance, thus hindering the overall system reliability. Furthermore, the communication networks on which AGC operation relies, may lead to increased vulnerabilities and risk for cyber attacks [2]. For example, a cyber attack may mask itself as noise in communication channels and influence the AGC system performance. Thus, there exists a need to study the combined effect of renewable resource uncertainty and communication channel noise on the function of the AGC system.

A thorough literature review of research in AGC is presented in [3]. The authors describe AGC schemes based on DC or AC power system formulation, optimal, centralized, decentralized and adaptive control. In addition, the authors discuss various aspects that arise from the integration of renewable resources. The combined effect of the customers' load demand and the renewable generation variability leads to a new net load curve for the ISOs. As a result, studies relating to AGC incorporating the dynamics of such systems are reported in the literature [4], [5]. In [6], the authors formulate the frequency regulation problem by viewing the future electric energy systems as a general dynamical system driven by disturbances and propose a modified AGC scheme that better responds to fast disturbances. In [7], the authors discuss issues related to very short term load prediction, security economic dispatch, variable generation management, and adaptive AGC unit tuning, to make the AGC system more efficient. The analysis of the system's behavior in the case an attacker gains access to the AGC signal and injects undesirable inputs to the system is studied in [8]; in this work, the authors propose the design of an optimal control strategy to destabilize a two-area power system in the case of a cyber attack in AGC.

As discussed earlier, given the changes in structure that power systems are undergoing, there is a need to investigate if the current AGC scheme is sufficient for meeting its objectives and to determine its limitations. To this end, this paper proposes a framework to evaluate the effects of uncertainties from renewable-based electricity resources and noise in the communication channels and to assess AGC system performance. The framework includes models for power system dynamics, the AGC system, and the aforementioned uncertainties. We use the framework to calculate several moments and approximate the probability distribution function of system variables, such as frequency. Additionally, we investigate whether or not the functionality provided by current AGC systems is appropriate for dealing with high levels of renewable-based electricity generation combined with noise in communication channels.

Power System Model

For the timescales of interest we choose a 4-state model for the synchronous generators that includes the mechanical equations and the governor dynamics. More specifically, for the ith synchronous generator, denote E'_{q_i} as the field flux linkage, δ_i as the rotor electrical angular position, ω_i as the rotor electrical angular velocity, and P_{SV_i} as the mechanical torque. Then, the ith generator can be modeled as

$$T'_{do_i}\frac{dE'_{q_i}}{dt} = -\frac{X_{d_i}}{X'_{d_i}}E'_{q_i} + \frac{X_{d_i}-X'_{d_i}}{X'_{d_i}}cos(\delta_i-\theta_i)$$
$$+ E_{fd0_i}, \tag{1}$$

$$\frac{d\delta_i}{dt} = \omega_i - \omega_s, \tag{2}$$

$$\frac{2H_i}{\omega_s}\frac{d\omega_i}{dt} = P_{SV_i} - \frac{E'_{q_i}}{X'_{d_i}}V_i sin(\delta_i-\theta_i) + \frac{X_{q_i}-X'_{d_i}}{2X'_{d_i}X_{q_i}}$$
$$V_i^2 sin(2(\delta_i-\theta_i)) - D_i(\omega_i-\omega_s), \tag{3}$$

$$T_{SV_i}\frac{dP_{SV_i}}{dt} = -P_{SV_i} + P_{C_i} - \frac{1}{R_{D_i}}\left(\frac{\omega_i}{\omega_s}-1\right), \tag{4}$$

where T'_{do_i}, H_i, E_{fd0_i}, X_{d_i}, X'_{d_i}, D_i, T_{SV_i}, and R_{D_i} are parameters that describe the machine characteristics; ω_s is the synchronous frequency; P_{C_i} is an input provided by the AGC system; and V_i and θ_i are the voltage magnitude and angle of bus i to which the machine is interconnected [9].

Unlike in traditional AGC modeling [10], we explicitly consider the network model; this way, we are capturing the effect that the network has on the overall closed-loop system dynamic behavior. Let P_{S_i} and P_{W_i} represent the real power generated from the synchronous generator and wind resource at bus i, and let P_{L_i} represent the real power load at bus i. Further, let Q_{S_i} and Q_{L_i} denote the reactive power supplied by the synchronous generator and demanded by the load at bus i, respectively. We assume that the reactive power generation of the wind resource is $Q_{W_i} = 0$. Then, we model the network using the standard nonlinear power flow formulation (see, e.g., [9]), and for the ith bus, we have that:

$$P_{S_i} + P_{W_i} - P_{L_i} = \sum_{k=1}^{n} V_i V_k\big(G_{ik}cos(\theta_i-\theta_k)$$
$$+ B_{ik}sin(\theta_i-\theta_k)\big)$$
$$Q_{S_i} - Q_{L_i} = \sum_{k=1}^{n} V_i V_k\big(G_{ik}sin(\theta_i-\theta_k)$$
$$- B_{ik}cos(\theta_i-\theta_k)\big),$$

where $G_{ik} + jB_{ik}$ is the (i,k) entry of the network admittance matrix and

$$P_{S_i} = \frac{E'_{q_i}}{X'_{d_i}}V_i sin(\delta_i-\theta_i) - \frac{X_{q_i}-X'_{d_i}}{2X'_{d_i}X_{q_i}}V_i^2 sin(2(\delta_i-\theta_i)),$$

$$Q_{S_i} = \frac{E'_{q_i}}{X'_{d_i}}V_i cos(\delta_i-\theta_i) - \frac{1}{X'_{d_i}}V_i^2 cos^2(\delta_i-\theta_i)$$
$$- \frac{1}{X_{q_i}}V_i^2 sin^2(\delta_i-\theta_i).$$

Assume that there are M balancing areas within an interconnected system and define $\mathscr{A} = \{1,\ldots,M\}$. For each $m \in \mathscr{A}$, we denote by $\mathscr{A}_m \subset \mathscr{A}$ the set of balancing areas that have transmission lines connected to area m. Also, we denote the actual power interchange out of area m to m' as $P_{mm'}$ and the actual frequency of area m as f_m. Then, we have

$$P_{mm'} = \sum_{\substack{l\in\mathscr{B}_{mm'}\\l'\in\mathscr{B}_{m'm}}} V_l V_{l'}\big(G_{ll'}cos(\theta_l-\theta_{l'}) + B_{ll'}sin(\theta_l-\theta_{l'})\big),$$
$$\tag{5}$$

where $\mathscr{B}_{mm'}$ ($\mathscr{B}_{m'm}$) is the set of nodes in area m (m') with tie lines to nodes in area m' (m). The actual frequency of area m is

$$f_m = \sum_{i\in\mathscr{B}_m} \gamma_i\left(f_{nom} + \frac{1}{2\pi}\frac{d\theta_i}{dt}\right), \tag{6}$$

where $\mathscr{B}_m$ is the set of buses in area m, f_{nom} is the nominal system frequency, each γ_i, $i \in \mathscr{B}_m$, represents some weighting factor and $\sum_{i\in\mathscr{B}_m}\gamma_i = 1$. Then, the area control error (ACE) for area m is given by

$$ACE_m = \sum_{m'\in\mathscr{A}_m}(P_{mm'} - P_{mm'_{sch}}) + b_m(f_m - f_{nom}), \tag{7}$$

where b_m is the bias factor for area m, which is positive, and $P_{mm'_{sch}}$ is the scheduled real power interchange out of area m to m'.

Define a new state for area m in the system, z_m, which, at steady state, is the total power generated in the balancing area m. Following [10, p. 352-355], it can be shown that the evolution of z_m is given by

$$\dot{z}_m = -z_m - ACE_m + \sum_{i\in\mathscr{G}_m} P_{S_i}, \tag{8}$$

where $\mathscr{G}_m$ is the set of generators in area m. Note z_m, the total generation in area m, decreases if ACE_m is positive, i.e., f_m is greater than the nominal frequency or the real power interchange is greater than that scheduled. Each generator $i \in \mathscr{G}_m$ participates in AGC with $P_{C_i} = \kappa_{m_i}z_m$, where κ_{m_i} for $i \in \mathscr{G}_m$ are the so-called participation factors and satisfy the relation $\sum_{i\in\mathscr{G}_m}\kappa_{m_i} = 1$ for $m \in \mathscr{A}$.

Consider a network with n nodes and I synchronous generators, and define $x = [x_1^T,\ldots,x_I^T]^T$, where $x_i = [E'_{q_i},\delta_i,\omega_i,P_{SV_i}]^T$. In addition, the vector of AGC signals is denoted by $u = [P_{C_1},\ldots,P_{C_I}]$, the vector of algebraic variables by $y = [y_1^T,\ldots,y_N^T]^T$, with $y_i = [\theta_i,V_i]^T$, the vector of loads (wind generation) by $P_L = [P_{L_1},\ldots,P_{L_n}]$ ($P_W = [P_{W_1},\ldots,P_{W_n}]$), and vector of AGC states by $z = [z_1,\ldots,z_M]$. Then, the system dynamic behavior is described by

$$\dot{x} = f(x,y,u), \tag{9}$$
$$\dot{z} = h(x,y,\dot{y},z), \tag{10}$$
$$u = k(z), \tag{11}$$
$$0 = g(x,y,P_L,P_W), \tag{12}$$

where the functions f, h, k, and g are continuously differentiable with respect to their arguments.

Incorporating Uncertainty

In the non-linear differential algebraic equation model described in (9)-(12) we consider two sources of uncertainty arising from wind-based generation and noise in communication channels. For the timescales of interest we assume that the disturbances due to the uncertainty sources introduce a small error and therefore we may linearize the system along a nominal trajectory $(x^\star, y^\star, u^\star, z^\star, P_W^\star, P_L^\star)$. Sufficiently small variations around the system nominal trajectory may be approximated by

$$\Delta\dot{x} = A_1(t)\Delta x + A_2(t)\Delta y + B_1(t)\Delta u, \tag{13}$$
$$\Delta\dot{z} = A_3(t)\Delta x + A_4(t)\Delta y + A_5(t)\Delta\dot{y} + A_6(t)\Delta z, \tag{14}$$
$$\Delta u = B_2(t)\Delta z, \tag{15}$$
$$0 = C_1(t)\Delta x + C_2(t)\Delta y + E_1(t)\Delta P_L + E_2(t)\Delta P_W, \tag{16}$$

where the matrices $A_1(t)$, $A_2(t)$, $A_3(t)$, $A_4(t)$, $A_5(t)$, $A_6(t)$, $B_1(t)$, $B_2(t)$, $C_1(t)$, $C_2(t)$, $E_2(t)$ and $E_2(t)$ are defined appropriately and evaluated along the nominal trajectory as the partial derivatives of the functions f, h, k, and g in (9)–(12) (see [11]). We assume the nominal trajectory is well behaved and admits an invertible Jacobian $C_2(t)$.

For the wind generation we assume a first order dynamical model, which yields an accurate relationship between the wind speed and the real power generated (see, e.g., [12], [13]). The active and reactive wind generation output around a nominal trajectory $(v_i^\star, P_{W_i}^\star)$ is given by

$$\Delta\dot{P}_{W_i} = \gamma_{1_i}\Delta P_{W_i} + \gamma_{2_i}\Delta v_i, \tag{17}$$

where Δv_i is the variation in the wind speed at bus i, and γ_{1_i} and γ_{2_i} are parameters that depend on the wind turbine characteristics. We model the variation in the wind speed as a stochastic process:

$$d\Delta v_i = a_i\,\Delta v_i\,dt + b_i\,dW_t, \tag{18}$$

where W_t is a Wiener process and a_i, b_i are parameters constructed based on a priori knowledge of the wind speed probability distribution.

Potential noise in communication channels may cause uncertainty in measurements of $\Delta P_{mm'}, \Delta f_m$ and ΔP_{S_i} which are used as feedback inputs for AGC. Let Γ be the vector containing all the $\Delta P_{mm'}, \Delta f_m$, and ΔP_{S_i}. We denote the measurements of Γ as $\hat{\Gamma}$,

$$\hat{\Gamma} = \Gamma + \eta, \tag{19}$$

where η represents the measurement noise, modeled as Gaussian white noise. The area control error as well as the AGC system is affected by η as may be seen in (7) and (8). Including this additional source of uncertainty in (14), we obtain

$$\Delta\dot{z} = A_3(t)\Delta x + A_4(t)\Delta y + A_5(t)\Delta\dot{y}$$
$$+ A_6(t)\Delta z + A_7(t)\eta. \tag{20}$$

In (16), as long as $C_2(t)$ is invertible, we can solve for Δy and then compute $\Delta\dot{y}$. With $\Delta P_L = 0$, we substitute Δu in (13) and obtain the following ordinary differential equation (ODE) model:

$$dX_t = AX_t dt + BdW_t, \tag{21}$$

where $X_t = [\Delta x, \Delta z, \Delta P_W, \Delta v]^T$, and A, B as defined in Appendix A.

The overall model, described in (21), is used to study the impact of the uncertainties on the system performance. To this end, we use the generator of the process X_t to calculate the statistics of the states of interest. Specifically, given a twice continuously differentiable function ψ, the generator of the process X_t is defined as (see, e.g. [14]):

$$(L\psi)(X) := \frac{\partial\psi(X)}{\partial X}AX + \frac{1}{2}\text{Tr}\left(B\frac{\partial^2\psi(X)}{\partial X^2}B^T\right). \tag{22}$$

The evolution of the expected value of $\psi(X)$ is governed by Dynkin's formula (see, e.g. [14]):

$$\frac{d\mathbb{E}[\psi(X((t))]}{dt} = \mathbb{E}[(L\psi)(X(t))], \tag{23}$$

where $\mathbb{E}[\cdot]$ is the expectation operator. For example, we may use (22) and (23) to obtain a formula for the evolution of the first and second moments of the system states:

$$\frac{d\mathbb{E}[X_t]}{dt} = A\mathbb{E}[X_t], \tag{24}$$
$$\frac{d\Sigma(t)}{dt} = A\Sigma(t) + \Sigma(t)A^T + BB^T, \tag{25}$$
$$\mathbb{E}[X_tX_t^T] = \Sigma(t) + \mathbb{E}[X_t]\mathbb{E}[X_t]^T. \tag{26}$$

By properly choosing function ψ, we may obtain ODEs that yield the desired moments of the dynamic/algebraic states (e.g. the expected values and variances of the load voltages and area frequencies). Therefore, we may study the effect of the uncertainties of wind-based generation and noise in communication channels on the AGC system.

Case Studies

We illustrate the proposed framework with a 4-bus test system, as depicted in Fig. 1, which contains two synchronous generating units in buses 1 and 4, one wind generation unit in bus 2 and load in bus 3. The machine, network, and load parameter values for the case studies are listed in Appendix B.
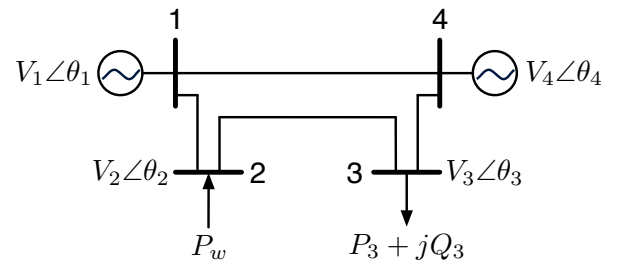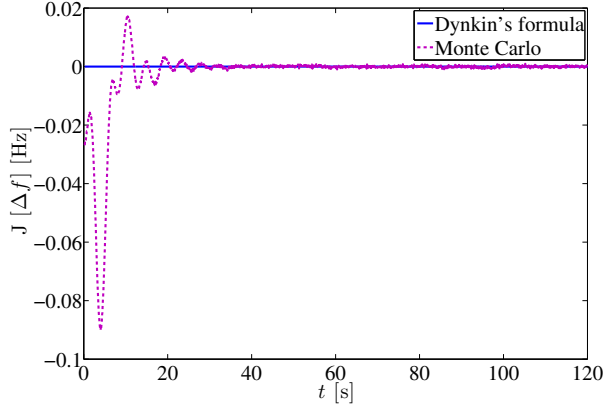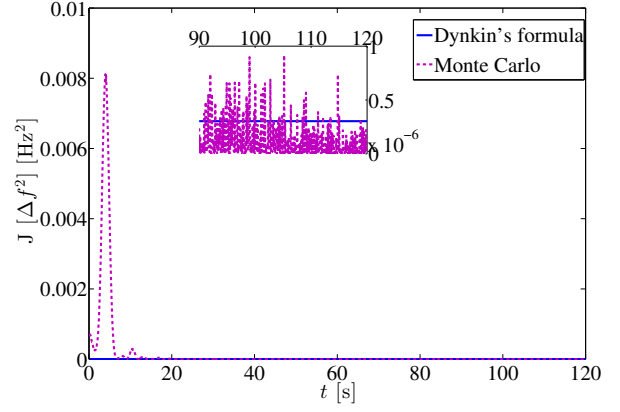

Fig. 1: One-line diagram of the 4-bus 2 machine system.

(a) Mean value of the frequency deviation.

(b) Second moment of the frequency deviation.

Fig. 2: Case (i): Uncertainty in wind-based generation

For simplicity, we consider one BA area for the system ($M = 1$) and choose the frequency bias factor to be $b_1 = 0.1$ MW/Hz. The AGC participation factors for each generator are $\kappa_1 = \frac{2}{3}$ and $\kappa_4 = \frac{1}{3}$. Unless otherwise noted, all quantities in the numerical results section are expressed in per unit (p.u.) with respect to 100 MVA as base power. We solve the power flow equations and the machine algebraic equations such that the wind generation in bus 2 is $P_W = 0.298$, the synchronous generator output in bus 4 is $P_{S_4} = 0.5$, the load in bus 3 is $P_3 + jQ_3 = 2.5 + j1.25$, the voltage magnitude in bus 1 is $V_1 = 1$ and bus 4 is $V_4 = 1.02$, with generator in bus 1 as the slack bus, picking up all power imbalances. We linearize the system of non-linear equations around the nominal point determined by solving the algebraic equations. The variation of the wind generation output in bus 2 is ΔP_W and its evolution is described by

$$\Delta \dot{P}_W = -0.1585 \Delta P_W + 0.0118 \Delta v, \qquad (27)$$

where the variation in the wind speed Δv is described by the stochastic process $d\Delta v = -6.2697 \Delta v dt + 10.9571 dW_t$.

We model potential noise in communication channels as a white noise process which we denote by η. Then, the ACE becomes

$$ACE = 0.1(\Delta f + \eta). \qquad (28)$$

In order to investigate the effectiveness of the AGC system, we choose to calculate the mean value and higher order moments of the frequency deviation as given in (6) by assigning equal weights to each bus, i.e., $\gamma_i = \frac{1}{4}$, $i = 1, \ldots, 4$, so we have

$$\Delta f = \frac{1}{8\pi} \left(\frac{d\Delta\theta_1}{dt} + \frac{d\Delta\theta_2}{dt} + \frac{d\Delta\theta_3}{dt} + \frac{d\Delta\theta_4}{dt} \right). \qquad (29)$$

The frequency deviation may also be expressed as a linear combination of the system states

$$\Delta f = C X_t, \qquad (30)$$

where $C = [\Sigma_1, \Sigma_2, \Sigma_3, \Sigma_4]$ and the matrices Σ_1, Σ_2, Σ_3 and Σ_4 are defined in Appendix A. Then $\mathbb{E}[\Delta f] = C\mathbb{E}[X_t]$ and $\mathbb{E}[\Delta f^2] = C\mathbb{E}[X_t X_t^T]C^T$. We observe that the elements of the vector C corresponding to the deviation of electrical angular speeds of generators 1 and 4 from ω_s, i.e., $\Delta\omega_1$ and $\Delta\omega_4$,
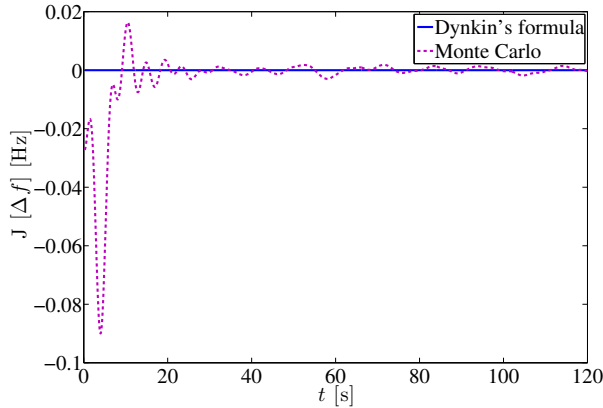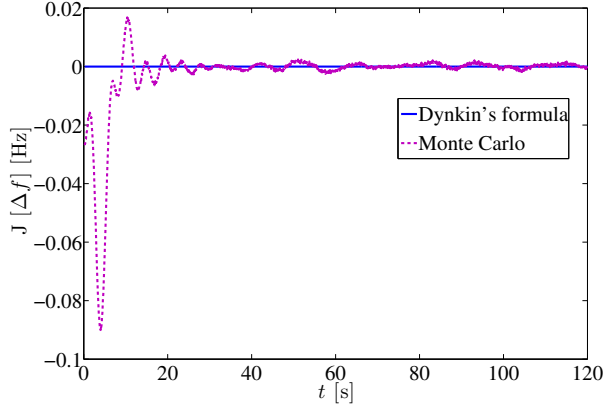

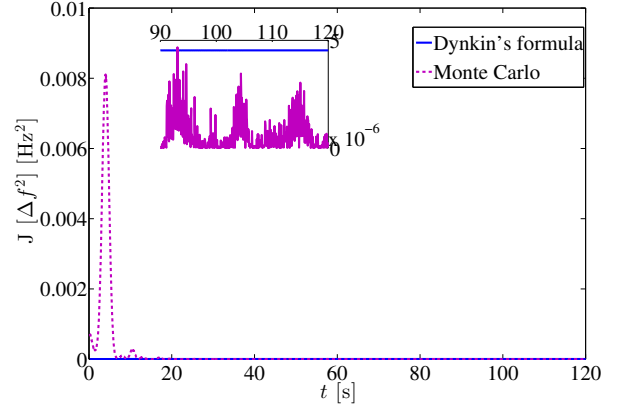(a) Mean value of the frequency deviation.
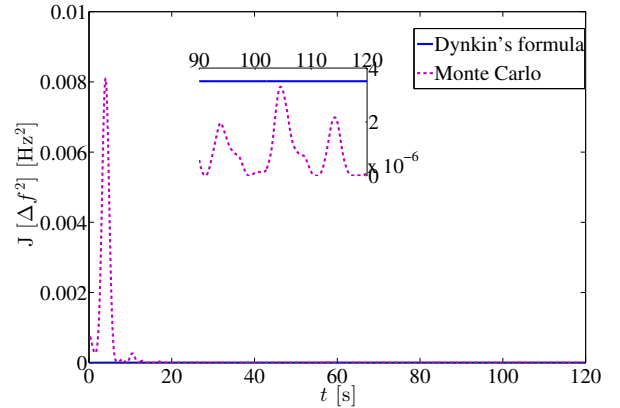
(b) Second moment of the frequency deviation.

Fig. 3: Case (ii): Noise in communication channels

4

(a) Mean value of the frequency deviation.

(b) Second moment of the frequency deviation.

Fig. 4: Case (iii): Uncertainty in wind-based generation and noise in communication channels

have the highest magnitude of 0.041. This is expected, since the frequency of the system is highly dependent on the electrical angular speed of generators.

We run three test cases in which we consider uncertainty in (i) the wind generation output, (ii) noise in communication channels and (iii) a combination of both. We validate the accuracy of the proposed framework by comparing the results with averaged Monte Carlo simulations, using the non-linear model given in (9)-(12). Figures 2-4 depict the mean value and the second moment of the frequency variation for the aforementioned three cases. The results obtained with the proposed framework are superimposed on those obtained by averaging the results of 1000 Monte Carlo simulations. The results provided by the analytical method, i.e., Dynkin's formula, match those obtained by averaging the results of repeated simulations. In this case, the AGC system meets its objective, since the mean value of the frequency variation $\mathbb{E}[\Delta f]$ converges to zero and the second order moment $\mathbb{E}[\Delta f^2]$ for all cases converges to a small value with magnitude of 10^{-6}. We may use the limits of $\mathbb{E}[\Delta f^2]$ and obtain an approximation for the standard deviation of Δf.

In case (iii) this approximation is higher than that in cases (i) and (ii), since $\lim_{t \to \infty} \mathbb{E}[\Delta f^2]_{(i)} = 3.04 \times 10^{-7}$, $\lim_{t \to \infty} \mathbb{E}[\Delta f^2]_{(ii)} = 3.51 \times 10^{-6}$ and $\lim_{t \to \infty} \mathbb{E}[\Delta f^2]_{(iii)} = 4.53 \times 10^{-6}$, as depicted in Figs 2b, 3b and 4b. This is expected since the combination of uncertainty in both wind-based generation and noise in communication channels is reflected in the AGC performance, thus higher variations of frequency are observed. However, the resulting variations in frequency are still sufficiently small that they lie within acceptable limits for the system's reliability. Moreover, we notice that noise in communication channels has a greater effect on the frequency deviation than wind-based generation. This is due to the wind turbine characteristics, as well as the features of the wind speed data. However, it is possible to choose another case for which the opposite effect may be observed.

Finally, we increase the wind penetration from the initial value $P_W = 0.298$ to $P'_W = \xi P_W$, where the parameter $\xi \in [1, 6]$ in increments of 0.5 and we investigate the impacts on the second moment of Δf. In order to represent the deepening penetration of wind generation and the increased level of variability in the output, we model the variation in the wind generation as

$$\Delta \dot{P}_W = -0.1585 \Delta P_W + 0.0118 \xi \Delta v. \tag{31}$$

We have $P'_W = \xi P_W \to \Delta P'_W = \xi \Delta P_W$, since the nominal point around which we linearize is now $P'^{\star}_W = \xi P^{\star}_W$. We observe that the second moment of the frequency deviation is higher as we increase the wind penetration levels, as shown in Fig. 5.

Concluding Remarks and Extensions

In this paper, we proposed a methodology for studying the impact on AGC system performance of uncertainty that arises from renewable-based power generation and noise in communication channels. Through the case studies, we show that
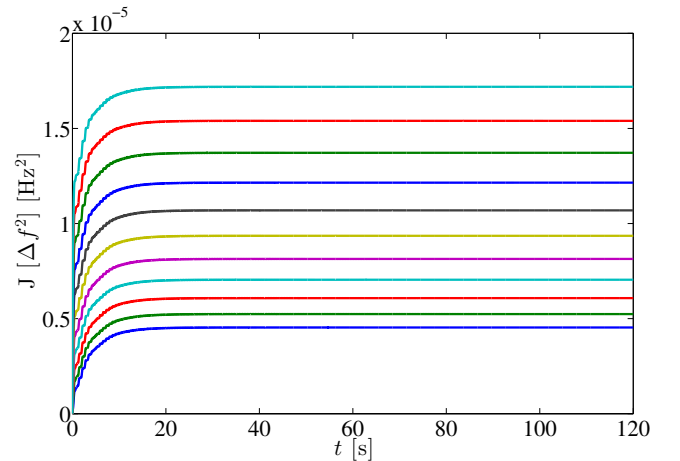

Fig. 5: Deepening wind penetration.

Dynkin's formula provides a good approximation of the system's true state, as validated with repetitive Monte Carlo simulations. Moreover, we show that in these cases the AGC system meets its objective despite the aforementioned sources of uncertainty. We also demonstrate that our model captures the higher uncertainty caused by the deepening penetration of renewable resources.

The proposed methodology may be used to detect, in a timely manner, the existence of a cyber attack, by computing the system frequency statistics and comparing them with those of the wind-based generation and communication channel noise. Furthermore, we may use it to determine which buses are more critical if noise is inserted in the measurements. In addition, we may use the proposed method to quantify the limiting amount of wind that may be integrated in the power system without violating the frequency performance metrics by obtaining upper bounds for the frequency variation, with the use of Chebyshev's inequality.

Appendix

A. Vectors and matrices definition

The vectors for the uncertainty models of wind resources (17) and noise in communications channels (18), the matrices for the ordinary differential set of equations in (21) and for the case study are defined as

$$\gamma_1 = [\gamma_{1_1}, \ldots, \gamma_{1_n}]^T, \quad \gamma_2 = [\gamma_{2_1}, \ldots, \gamma_{2_n}]^T,$$
$$a = [a_1, \ldots, a_n]^T, \quad b = [b_1, \ldots, b_n]^T,$$
$$A = \begin{bmatrix} A_{11} & A_{12} & A_{13} & A_{14} \\ A_{21} & A_{22} & A_{23} & A_{24} \\ A_{31} & A_{32} & A_{33} & A_{34} \\ A_{41} & A_{42} & A_{43} & A_{44} \end{bmatrix}, \quad B = \begin{bmatrix} B_{11} \\ B_{21} \\ B_{31} \\ B_{41} \end{bmatrix}, \text{ with}$$
$$A_{11} = A_1 - A_2 C_2^{-1} C_1, \quad A_{12} = B_1 B_2,$$
$$A_{13} = -A_2 C_2^{-1} E_2, \quad A_{14} = 0_{4I-1 \times n},$$
$$A_{21} = A_3 - A_5 C_2^{-1} C_1 A_1 +$$
$$\quad A_5 C_2^{-1} C_1 A_2 C_2^{-1} C_1 - A_4 C_2^{-1} C_1,$$
$$A_{22} = -A_5 C_2^{-1} C_1 B_1 B_2 + A_6,$$
$$A_{23} = A_5 C_2^{-1} C_1 A_2 C_2^{-1} E_2 - A_4 C_2^{-1} E_2 - A_5 C_2^{-1} E_2 \gamma_1,$$
$$A_{24} = A_5 C_2^{-1} E_2 \gamma_2, \quad A_{31} = 0_{n \times 4I-1}, \quad A_{32} = 0_{n \times m}$$
$$A_{33} = \gamma_1, \quad A_{34} = \gamma_2, \quad A_{41} = 0_{n \times 4I-1}, \quad A_{42} = 0_{n \times m},$$
$$A_{43} = 0_{n \times n}, \quad A_{44} = a, \quad B_{11} = 0_{4I-1 \times 1}, \quad B_{21} = A_7,$$
$$B_{31} = 0_{n \times 1}, \quad B_{41} = b, \quad \Phi = \frac{1}{8\pi}[1, 0, 1, 0, 1, 0, 1, 0],$$
$$\Sigma_1 = \Phi(C_2^{-1} C_1 A_1 + C_2^{-1} C_1 A_2 C_2^{-1} C_1)$$
$$\Sigma_2 = \Phi C_2^{-1} C_1 B_1 B_2$$
$$\Sigma_3 = \Phi(C_2^{-1} C_1 A_2 C_2^{-1} E_2 - C_2^{-1} E_2 \gamma_1)$$
$$\Sigma_4 = \Phi C_2^{-1} E_2 \gamma_2$$

B. Parameter values for the 4-bus system

The system MVA base is 100; the synchronous speed, $\omega_s = 377 rad/s$; the machines shaft inertia constants, $H_1 = 23.64$ and $H_4 = 6.4$; the machines damping coefficient $D_1 = 0.0125$, $D_4 = 0.0068$, the machine impedances, $X_{d_1} = 0.146$, $X_{d_4} = 0.8958$, $X'_{d_1} = 0.0608$, $X'_{d_4} = 0.1198$, $X_{q_1} = 0.0969$ and $X_{q_4} = 0.8645$; the governor droops $R_{D_1} = R_{D_4} = 0.05$; and the time constants $T'_{do_1} = 8.96$, $T'_{do_4} = 6.0$ and $T_{SV_1} = T_{SV_4} = 2$. The network impedances between bus i and j are denoted by Z_{ij}, so we have: $Z_{12} = 0.0101 + j0.0504$, $Z_{14} = Z_{23} = 0.0074 + j0.0372$, $Z_{34} = 0.0127 + j0.0636$.

REFERENCES

[1] GAO-11-117, "Electricity grid modernization: Progress being made on cyber security guidelines, but key challenges remain to be addressed," *Government Accountability Office (GAO)*, January 2011.

[2] Y. Huang, A. A. Cardenas, and S. Sastry, "Understanding the physical and economic consequences of attacks on control systems," *Elsevier, International Journal of Critical Infrastructure Protection*, 2009.

[3] I. Ibraheem, P. Kumar, and D. P. Kothari, "Recent philosophies of automatic generation control strategies in power systems," *IEEE Transactions on Power Systems*, vol. 20, no. 1, pp. 346–357, 2005.

[4] D. H. Curtice and T. W. Reddoch, "An assessment of load frequency control impacts caused by small wind turbines," *IEEE Transactions on Power Apparatus and Systems*, vol. PAS-102, no. 1, pp. 162–170, 1983.

[5] J. L. Rodriguez-Amenedo., S. Arnalte, and J. C. Burgos, "Automatic generation control of a wind farm with variable speed wind turbines," *IEEE Transactions on Energy Conversion*, vol. 17, no. 2, pp. 279–284, 2002.

[6] Q. Liu and M. D. Ilic, "Enhanced automatic generation control (e-agc) for future electric energy systems," in *IEEE Power and Energy Society General Meeting*, 2012, pp. 1–8.

[7] D. Chen, S. Kumar, M. York, and L. Wang, "Smart automatic generation control," in *IEEE Power and Energy Society General Meeting*, 2012, pp. 1–7.

[8] P. Esfahani, M. Vrakopoulou, K. Margellos, J. Lygeros, and G. Andersson, "A robust policy for automatic generation control cyber attack in two area power network," in *49th IEEE Conference on Decision and Control (CDC)*, 2010, pp. 5973–5978.

[9] P. W. Sauer and M. A. Pai, *Power System Dynamics and Stability*. Upper Saddle River, NJ: Prentice Hall, 1998.

[10] A. Wood and B. Wollenberg, *Power Generation, Operation, and Control*. New York, NY: Wiley, 1996.

[11] A. D. Domínguez-García, *Models for Impact Assessment of Wind-Based Power Generation on Frequency Control*. in Control and Optimization Methods for Electric Smart Grids, Power Electronics and Power Systems, M. Ilić and A. Chakrabortty, Springer, 2012.

[12] H. A. Pulgar-Painemal and P. W. Sauer, "Towards a wind farm reduced-order model," *Electric Power Systems Research*, vol. 81, no. 8, pp. 1688 – 1695, 2011.

[13] Y. C. Chen and A. D. Domínguez-García, "A method to study the effect of renewable resource variability on power system dynamics," *IEEE Transactions on Power Systems*, vol. 27, no. 4, pp. 1978–1989, 2012.

[14] B. Øksendal, *Stochastic Differential Equations: An Introduction with Applications*, ser. Universitext (1979). Springer, 2003.